ORNL
MASTER COPY DATE ISSUED AUG 0 8 1986

ORNL/TM-9950

ornl

OAK RIDGE
NATIONAL
LABORATORY

MARTIN MARIETTA

Turbulent Dispersion Results from Gel-Sphere Processes and Application to Centrifugal Contactors

P. A. Haas

OPERATED BY
MARTIN MARIETTA ENERGY SYSTEMS, INC.
FOR THE UNITED STATES
DEPARTMENT OF ENERGY

Printed in the United States of America. Available from
National Technical Information Service
U.S. Department of Commerce
5285 Port Royal Road, Springfield, Virginia 22161
NTIS price codes—Printed Copy: A04; Microfiche A01

This report was prepared as an account of work sponsored by an agency of the United States Government. Neither the United States Government nor any agency thereof, nor any of their employees, makes any warranty, express or implied, or assumes any legal liability or responsibility for the accuracy, completeness, or usefulness of any information, apparatus, product, or process disclosed, or represents that its use would not infringe privately owned rights. Reference herein to any specific commercial product, process, or service by trade name, trademark, manufacturer, or otherwise, does not necessarily constitute or imply its endorsement, recommendation, or favoring by the United States Government or any agency thereof. The views and opinions of authors expressed herein do not necessarily state or reflect those of the United States Government or any agency thereof.

ORNL/TM-9950
Dist. Category UC-86

Consolidated Fuel Reprocessing Program

TURBULENT DISPERSION RESULTS FROM GEL-SPHERE PROCESSES AND APPLICATION TO CENTRIFUGAL CONTACTORS

P. A. Haas
Chemical Technology Division

Date Published: July 1986

Prepared by the
OAK RIDGE NATIONAL LABORATORY
Oak Ridge, Tennessee 37831
operated by
MARTIN MARIETTA ENERGY SYSTEMS, INC.
for the
U.S. DEPARTMENT OF ENERGY
under Contract No. DE-AC05-84OR21400

CONTENTS

ACKNOWLEDGMENTS v

ABSTRACT vii

1. INTRODUCTION 1
   1.1 Gel-Sphere Processes and Role of Drop Formation 1
   1.2 Theory of Turbulent Dispersion Mechanism 2

2. DESCRIPTION OF THREE TURBULENT DISPERSION DEVICES 5

3. DETERMINATION AND REPRESENTATION OF DROP-SIZE DISTRIBUTIONS 9

4. EMPIRICAL CORRELATION OF RESULTS 13

5. CORRELATION OF RESULTS BY TURBULENT DISPERSION THEORY 21

6. COMPARISONS OF CORRELATIONS WITH LITERATURE DATA 27

7. APPLICATION TO ANNULAR MIXING FOR CENTRIFUGAL CONTACTORS 31

8. RESULTS AND CONCLUSIONS 35

REFERENCES 37

NOMENCLATURE 39

ACKNOWLEDGMENTS

R. D. Arthur, V. L. Fowler, A. D. Ryon, and J. S. Vavruska made important contributions to the concepts and testing of the turbulent dispersion devices described in Sect. 1.

ABSTRACT

Drop sizes for turbulent dispersion of aqueous solutions in organic liquids were determined and correlated for three types of dispersion devices, (1) flow in tubes, (2) motionless mixer units, and (3) a rotating annular disperser with couette flow. Empirical correlations based on dimensional analyses were useful for application of these devices to gel-sphere processes. The results support the Kolmorogoff theory of turbulence as a dispersion mechanism for a range of 10^4 for the rate of energy dissipation. Application of the results to centrifugal contactors for solvent extraction indicates average sizes of 110 to 310 μm for aqueous drops in a continuous phase of 30% tributyl phosphate (TBP) in a hydrocarbon diluent.

1. INTRODUCTION

Three different devices using controlled velocities of organic liquids were applied to disperse aqueous solutions as drops. One consisted of simple tubes of small diameters. A second contained motionless mixer units inside larger tubes. The third employed couette flow of the organic liquid between a cylindrical rotor and a stationary cylinder.

These devices were applied to gel-sphere processes in which the liquid drops are converted into solid gel spheres of hydrated metal oxides. The gel-sphere products are good, strong spheres and allow good measurement of the sphere and the drop-size distributions. The drop diameters must be controlled and predictable to allow preparation of product spheres of the desired sizes. Empirical correlations were determined for application to the gel-sphere processes.

The theory of turbulent dispersion based on eddy velocities has been developed by Kolmorogoff[1], Hinze[2], and others. Davies[3] reviewed this theory and the agreement of theory with four types of dispersion devices for energy dissipation rates of 6 to 400,000 W/g. The gel-sphere results for drop-size distributions are for energy dissipation rates of 10^{-3} to 1.5 W/g. These combined results support the theory of turbulence as the dispersion mechanism over a range of 10^9 for the rate of energy dissipation.

The turbulent dispersion with couette flow is the mechanism for mixing in an advanced design of centrifugal contactors for solvent extraction. The theory of turbulence is applied to predict drop sizes and mixing power for centrifugal contactors as developed at Oak Ridge National Laboratory (ORNL).

1.1 GEL-SPHERE PROCESSES AND ROLE OF DROP FORMATION

A limited description of gel-sphere processes is given here to explain the drop formation conditions and results. Some detailed descriptions of chemical flowsheet conditions and equipment and procedures have been published. Depending on the mechanism of gelation, the drops must be dispersed into trichloroethylene (TCE), 2-ethyl-1-hexanol (2EH), silicone oil, NH_3 gas or solution, or other fluids. These gel-sphere processes have been described by Haas et al.[4,5], Haas and Clinton[6], Bischoff et al.[7], and Zimmer et al.[8].

The preparation of gel-spheres by processes developed at ORNL and elsewhere is based on the conversion of liquid drops into solid gel spheres of hydrated metal oxides. Each liquid or broth* drop must contain the amount of metal needed in one product

*Depending on the gel-sphere process, the feed liquid may contain colloidal oxides, metal salts, organic polymers, metals in complexed or hydrolyzed form, or other chemicals. This feed to the gelation step may be termed a "broth."

sphere. The diameters of the drops determine the diameters of the product spheres. The solidification of the drop may result from mass transfer of NH_3, NH_4OH, HNO_3, H_2O, or from chemical reactions inside the drop. Mass transfer from the drop also occurs during washing to remove solutes, drying to remove H_2O and other volatile constituents, and thermal treatments. The product spheres are generally much smaller than the liquid drops. There is no significant loss of metal during these process operations, and the metal concentrations in the liquid drop and the product sphere are accurately measured; therefore, the diameter ratio of liquid drop:product sphere is accurately known.

The gel-sphere products are usually excellent, strong spheres and allow a convenient and accurate measurement of the liquid drop sizes. The complete batch of product can be used as a sample, or procedures that ensure representative sampling can be used. In this way, many of the uncertainties involved in measuring liquid-drop diameters in a second liquid are avoided. The possibility of coalescence or of an additional secondary dispersion before solidification occurs must be considered.

Some of the results reported in this paper were obtained from many hours of operation to prepare test batches of nuclear reactor fuels. These results demonstrated good reproducibility of the drop formation procedures. All the turbulent disperser results were for dispersion of aqueous drops into organic liquids; the gelation procedures using aqueous NH_4OH solutions were not practical for small gel spheres.

Controlled and uniform product diameters are important to many applications of gel-sphere processes. Procedures that gave excellent size uniformity for drops of 500 to 5000 μm[9] were not practical for smaller drops. Simple mixing using agitators at controlled speeds gave control of the average diameters, but the uniformity of drop size was poor. The turbulence produced by an agitator is obviously both nonuniform and nonisotropic. The results in this paper are for three dispersers that were expected to provide a more uniform turbulence than that from agitators.

1.2 THEORY OF TURBULENT DISPERSION MECHANISM

The dispersion of one liquid into another as a result of turbulence has been discussed by a large number of authors. A theory of homogeneous, isotropic turbulence was developed by Kolmogoroff[1]. The dispersion results from the turbulent fluctuations or eddies and the fluctuation velocities are determined by the rate of energy dissipation. The pressure from the fluctuation velocities is opposed by the surface tension holding the drop together. The maximum drop size that is stable with respect to further dispersion is given by

$$d_{\max} = C_2 \left(\frac{\gamma}{\rho}\right)^{0.6} P^{-0.4} \ , \tag{1}$$

where the constant, C_2, is dimensionless and has a value near one. The viscosity of the liquid drop was neglected for the theory used to derive Eq. (1), and the viscous forces inside the drop can also contribute to the resistance to breakup. Davies[3] proposed adding a viscous force term to the interfacial tension as follows:

$$d_{\max} = C_2\left(\gamma + \frac{\mu_d v}{4}\right)\rho^{0.6}P^{-0.4} \quad . \tag{2}$$

Substitution of equations for P in Eq. (1) can give many of the relationships in the literature for $d_{\max}$ versus Weber number (We), Reynolds number (Re), and velocities or rpm. The interfacial tension would not normally appear in P, and an almost universal result is

$$d_{\max} \propto (We)^{-0.6} \quad . \tag{3}$$

Davies[10] has given a more complete discussion of isotropic turbulence and a comparison of the theory of turbulent dispersion with experimental data.

2. DESCRIPTION OF THREE TURBULENT DISPERSION DEVICES

The theory of turbulent dispersion mechanism and the gel-sphere process requirements indicated a need for a controlled and uniform turbulence. Also the flow through the turbulent zone should be positive and the holdup time limited so that the dispersed drops can solidify or gel without continued exposure to the turbulence. Dispersion devices with these attributes should give improved uniformity of drop-size distribution as compared to previous results with dispersion by an agitator. The dispersion by an agitator also gave some dumbbell or clumped spheres, which were believed to result from recycle of partly solidified spheres through the agitator. The three dispersion devices tested in this study were selected from these considerations.

Flow in an open tube provides a well-defined flow regime and is the simplest of the three types of dispersers studied. The tube is characterized by a single dimension, the diameter, D. The system Weber number and the Reynolds number are unambiguous. The aqueous phase to be formed into drops was introduced through capillaries at velocities that were usually within a factor of 4 of the organic velocity, and the diameter of this capillary was not a significant variable. The first tests were done with glass units (Fig. 1), but later tests were more commonly performed with hypodermic needles brazed into stainless steel tubing.

The motionless or static mixers used in these studies were 0.335- to 0.80-cm-ID tubes containing 21 mixing elements.* These Kenics mixers have 180°-helical elements of alternating right- and left-hand twists with each element length equal to 1.5 diam (Fig. 2). The elements divide the tube into two semicircular flow channels. The alternating twist elements are joined 90° out-of-phase so that each flow from one element is split between the two channels of the next element.

To make empirical correlations, these motionless mixers were characterized by the ID, and the average velocities were calculated using these IDs. The empirical constants should not be used for other static mixers with mixing elements of different proportions. The true velocities would be much higher than the average velocities calculated using the ID, because the mixing elements both reduce the cross section for flow and increase the path length. The hydraulic diameters of the flow channels would be smaller than the ID. The void volumes inside the tube were measured by water displacement and were from two-thirds to five-sixths of the volume calculated using the nominal ID. Calculations from the weights of the dry units also indicated that the mixing elements occupied one-third to one-sixth of the tube volume. This high-volume fraction of mixing elements agrees with the visual appearance of these small units and would probably not apply to larger units.

*Kenics Corporation, North Andover, Massachusetts, Model Series 37.

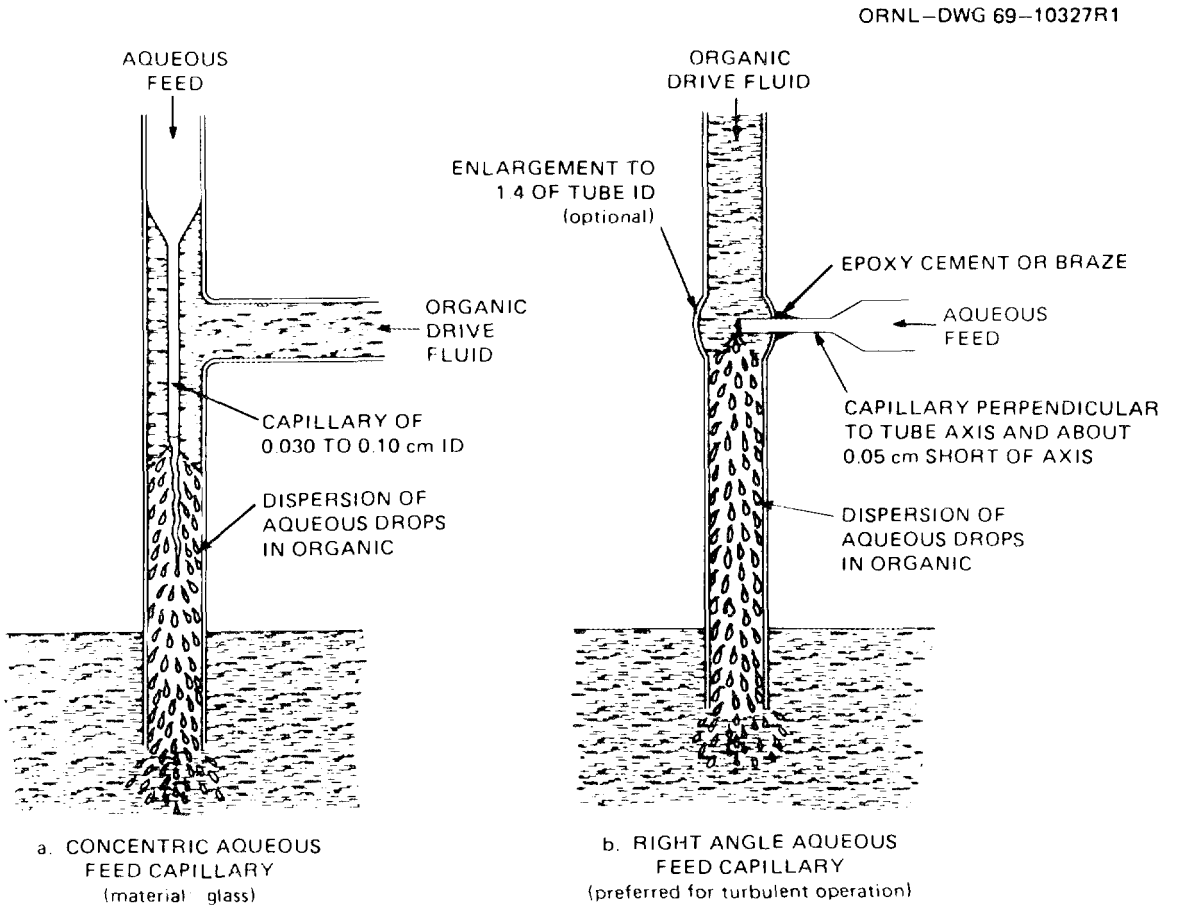

Fig. 1. Schematic views of two-fluid nozzles.

The third dispersion device may be called a couette flow or annular disperser. A shear field can be generated in the annulus between two cylinders rotating at different speeds. The flow patterns for such a thin annulus are termed couette flow. This type of disperser was tested as a possible means of preparing UO_3 spheres via internal gelation by using a motor-driven rotor mounted inside a stationary cylinder (Fig. 3). The bottom of the rotor was provided with an enlarged diameter to pump fluid by centrifugal action. The first test unit had conical surfaces for the entire rotor and stator at a 1.5° angle. Thus, the annulus thickness could be varied by simply moving the stator up or down with respect to the rotor. However, this arrangement gave an excessive pumping rate of the continuous phase as well as a variable shear field along the annulus. Experimental data from the conical unit were used to evaluate the effect of annulus thickness, but an annulus of uniform diameter (no taper) appeared to provide better control of drop diameter. The hydraulic diameter of the flow channel, D, would be twice the annulus thickness for the couette disperser. The other dimension, ID, was taken as the rotor diameter. In addition to the D/ID term, the rotor diameter is used to calculate the velocity: $V = \pi(\mathrm{ID})\ (\mathrm{rpm}/60)$.

For all the gel-sphere tests of turbulent disperser devices, the fraction of dispersed phase and the size of the aqueous feed inlet did not have any significant effects on the

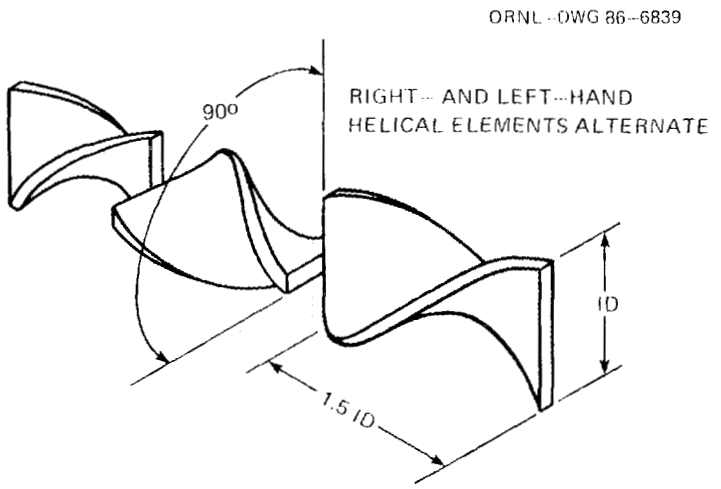

MODEL NO.	ID,cm	L=31.51D cm	NUMBER OF ELEMENTS	VOID VOLUME / OPEN TUBE VOLUME
37-03-062	0.335	10.6	21	2/3
37-04-065	0.493	15.5	21	...
37-06-109	0.80	25.5	21	5/6

Fig. 2. Kenics static mixers for this study.

drop diameters. The ratio of continuous- or organic-phase flow rates to the aqueous flow rates were usually from 40:1 to 100:1, with a few tests with ratios of 25:1 to 40:1. These high ratios were necessary to provide the water extraction capacity for external gelation or to provide heat capacity for internal gelation. The aqueous velocities in the feed inlets were commonly from 0.25 to 1 times the organic velocities for the simple tube and static mixer dispersers and were much lower for the aqueous feed inlet to the couette disperser. The observed drop sizes were always smaller (usually much smaller) than the ID of the aqueous feed inlet and were therefore not determined by this diameter.

ORNL DWG 81-15453R

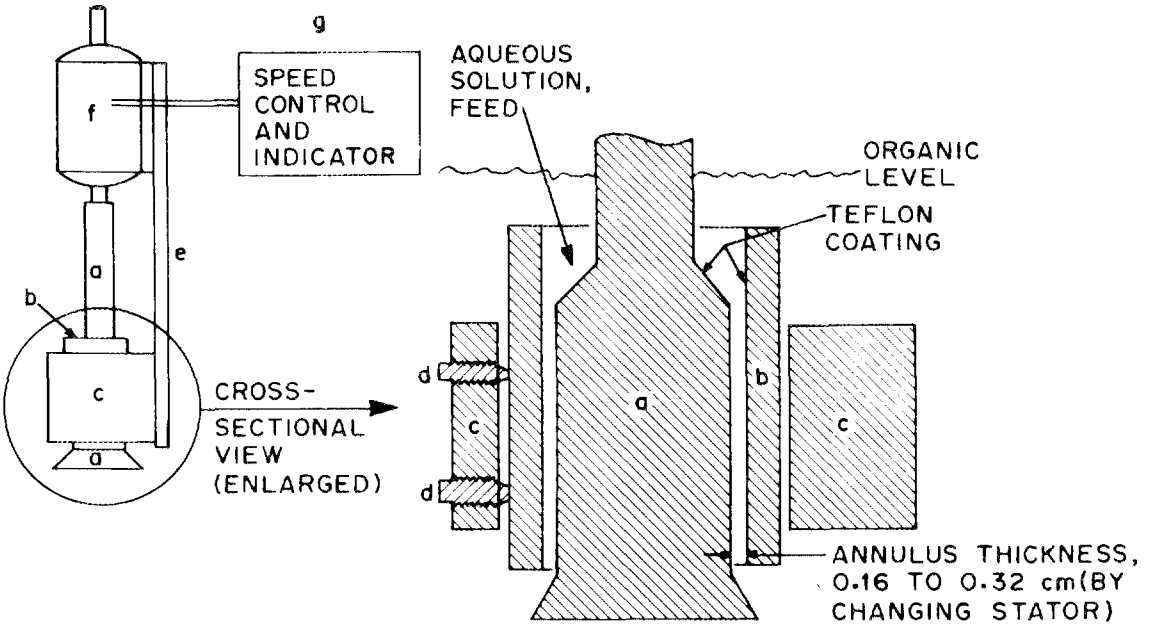

a. ROTOR, STAINLESS STEEL WITH TEFLON COATING, 3.18-cm OD
b. STATOR, STAINLESS STEEL WITH TEFLON COATING ON ID
c. SUPPORT BLOCK (BOLTED TO MOTOR BRACKET)
d. SET SCREWS TO CENTER STATOR; THREE SETS OF TWO
e. MOTOR BRACKET
f. SERVOMOTOR
g. MOTOR SPEED CONTROL

Fig. 3. Couette disperser apparatus.

3. DETERMINATION AND REPRESENTATION OF DROP-SIZE DISTRIBUTIONS

Three different areas of size information and calculation are important to these gel-sphere results. These are the size measurements for the product spheres, the calculation of drop sizes from the product sizes, and the representation of size data for correlation.

The principal size measurements for the dry product spheres were by standard test sieves and procedures (U.S. Sieve Series). Large batches of spheres for nuclear fuel samples were blended and sampled by riffling procedures. As compared to materials of irregular shape, the spheres were free-flowing and allowed good size separations. For some compositions, the smallest spheres showed some tendency to be present as small clusters or to be weakly attached to a larger sphere. The significance of such fines on a weight basis is small.

The known concentrations of metal in the liquid before gelation and in the product sphere allow a simple and accurate calculation of diameter ratio or shrinkage factor, SF.

$$\mathrm{SF} = \frac{\text{Diameter of drop}}{\text{Diameter of product}} = \left(\frac{\text{Concentration of product}}{\text{Concentration of liquid feed}}\right)^{1/3} . \tag{4}$$

This equation is a simple material balance for thorium, uranium, or other metals that remain in the sphere without significant losses. The products were usually oxides (ThO_2, UO_3, or UO_2) of high purity so that the product concentration was determined by measuring the sphere density. For a single-size fraction of U.S. Sieve Series, the spheres poured into a graduate slowly and tapped lightly would pack to 38% void volume, and the sphere density would be the (bulk density)/0.62. The ThO_2 gel spheres can be sintered to the theoretical density (10 g/cm^3) of ThO_2. An example of a shrinkage calculation for dense ThO_2 is

Feed concentration: 2.50 *M* Th.

Product concentration: $\frac{(10)(1000)}{264} = 37.88\ M\ \mathrm{Th}$.

$$\mathrm{SF} = \frac{\text{Diameter of drop}}{\text{Diameter of product}} = \left(\frac{37.88}{2.50}\right)^{1/3} = 2.47 .$$

For gel-sphere products, the weight or mass average diameter and the yield within a range of diameters are pertinent. The exact distribution of very large or fine sizes is not important. A normal distribution has the obvious limitation that it may indicate negative

sizes that are physically impossible. A log-normal distribution does not have this limitation and is mathematically convenient to use. The use of log-probability paper provides a simple test of the suitability of the log-normal fit and permits a simple determination of the mean and standard deviation. If more than 80% of the spheres give a straight line on log-probability paper, d and σ are determined from the line, and the nonlinear ends of the plot are ignored. The mean of the drop sizes on a weight or mass basis is this d from the log-probability plot times the shrinkage factor, SF. The standard deviations, $\sigma = d_{84}/d$, for log-normal distributions are the same for the product spheres and the drops.

Typical examples are shown of sieve analysis of product spheres for two tests each of the three types of dispersers (Fig. 4). The product, d and σ, are determined from these curves. The average drop diameters are calculated using the shrinkage factor, SF, from concentrations as previously described.

Size distributions for the three types of dispersers were compared, as were some literature size distributions using the σ's for log-normal distributions. Nearly all of the σ's were from 1.21 to 1.50, with 1.28 to 1.35 as the most typical values. While clear quantitative conclusions are uncertain, the following qualitative conclusions were indicated. It appears that the smallest σ values or best uniformity for this type of dispersion (an equilibrium drop-size distribution in a uniform turbulence) are $\sigma = 1.28$; lower values are not reproducible. Conditions that do not achieve an equilibrium size distribution or a uniformity of turbulence give larger σ values. The static mixers provide the best uniformity (lowest σ values) (Fig. 4). Equally good results can be obtained with the couette disperser, but conditions that include short exposure times (i.e., high continuous-phase pumping rates) yield larger σ values. The open-tube data show less uniformity of size, with σ values ranging from 1.3 to 1.4 (Fig. 4).

ORNL DWG 83-1033R

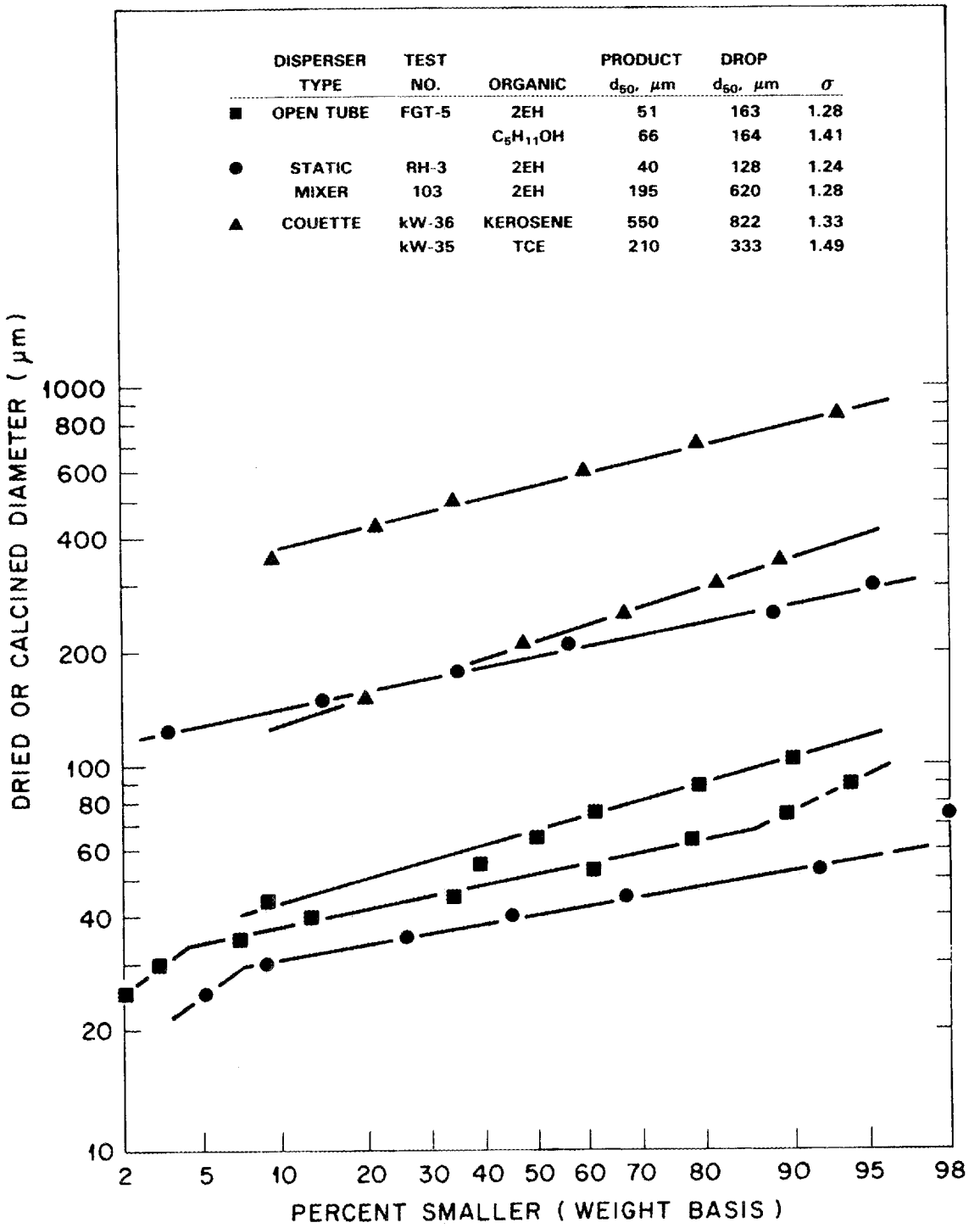

Fig. 4. Size distributions for oxide spheres with drop formation by several dispersers.

4. EMPIRICAL CORRELATION OF RESULTS

Correlation of drop-formation data were needed for convenient operation of gel-sphere processes. The empirical correlations were based on a dimensional analyses with an exponential relationship. Dimensionless ratios of two densities and of a density to a density difference appeared in the dimensional analyses result, but these ratios either were not significant or the data were not able to show their effect. With these density ratios omitted, the following three arrangements of the results were used:

$$\frac{d}{D} = C_1\left(\frac{D\rho V^2}{\gamma}\right)^a\left(\frac{D\rho V}{\mu_c}\right)^b\left(\frac{\mu_d}{\mu_c}\right)^c\left(\frac{D}{ID}\right)^g , \tag{5}$$

$$\frac{d}{ID} = C_1\left(\frac{ID\rho V^2}{\gamma}\right)^a\left(\frac{ID\rho V}{\mu_c}\right)^b\left(\frac{\mu_d}{\mu_c}\right)^c\left(\frac{D}{ID}\right)^{g+1+a+b} , \tag{6}$$

$$d = C_1(V^{a+b}\gamma^{-a}D^{1+a+b+g}ID^{-g}\mu_c^{-b-c}\mu_d^c\rho^{a+b}) . \tag{7}$$

The dimensionless numbers with the exponents a and b are, respectively, the system Weber numbers and the Reynolds numbers. The first arrangement, Eq. (5), was applied to the simple tube and to the couette disperser. The second arrangement, Eq. (6), was used for the static mixer to indicate that the correlation uses the tube ID to calculate average velocities and as the diameters in the Weber and Reynolds numbers. The third arrangement, Eq. (7), indicates a logical procedure for examining the fit and determining exponents.

The first test of the experimental data is to plot log d versus log V for data, with d and V as the only variables [one disperser and a single pair of fluids (Fig. 5)]. All of the well-defined lines were well represented by straight lines with slopes of -1.4 to -1.6. These included several dispersers and several fluid pairs for both the open tube and the couette disperser. Some small sets of open tube data showed slopes of -1 to -1.6, and some static mixer slopes were from -0.8 to -2.1. However, all of these values that were outside the range -1.4 to -1.6 were either for a narrow range of velocities or were very dependent on a single extreme data point. Allowing for these limitations, all the data could be adequately represented by slopes of $2a+b = -1.5$. Using this value for $2a+b$, log $dV^{1.5}$ was plotted versus log D or log ID with other variables constant; that is, data for the same pair of fluids in dispersers of different diameters. For the simple tube with D as the only diameter variable, the slopes were $2.5 - a = 3.15$ or $a = -0.65$. This gives $b = -0.2$. The above procedure has determined a coefficient for the Weber number, $a = -0.65$, without use of the surface tension or viscosity data. Most of the differences between fluids is accounted for by the effects of surface tension, but high viscosities also

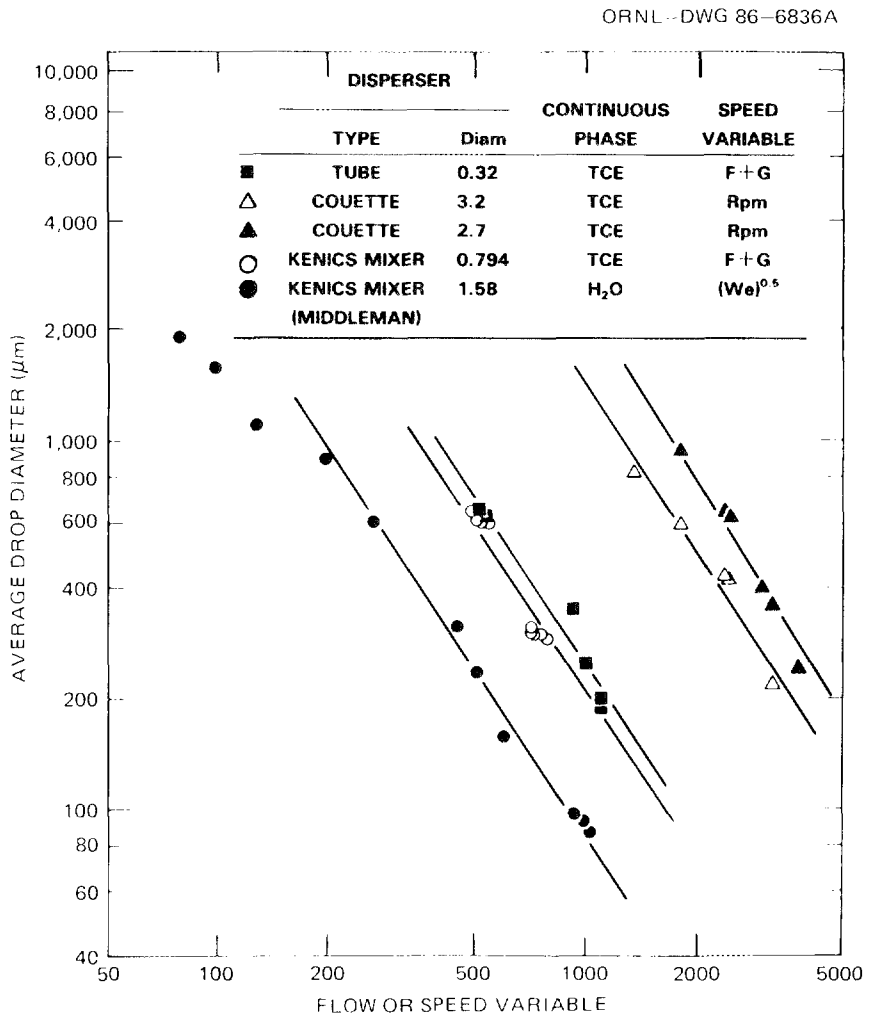

Fig. 5. Drop diameter vs velocity for turbulent dispersion.

have significant effects. The largest viscosity differences indicate values of $c = 0.4$ or 0.5 while the smaller differences are indeterminant. The dependence of d on ID for the couette disperser was used to estimate the exponent, g. For the static mixer, the D/ID term was combined with C_1 as an empirical coefficient. The density of the continuous phase appears in both Weber and Reynolds numbers. The effects of the discontinuous phase density in terms of density ratios or a density difference ratio were not detectable in our data, and these terms were dropped from Eqs. (5) through (7).

The final empirical correlations are as follows:

1. The simple tubes or turbulent two-fluid nozzles with TCE, 2EH, and isoamyl alcohol (iAA) gave

$$\frac{d}{D} = 15(\mathrm{We})^{-0.65}(\mathrm{Re})^{-0.2}\left(\frac{\mu_d}{\mu_c}\right)^{0.5} . \tag{8}$$

2. The static mixers with TCE and 2EH gave

$$\frac{d}{ID} = 1.2(\mathrm{We})^{-0.65}(\mathrm{Re})^{-0.2}\left(\frac{\mu_d}{\mu_c}\right)^{0.5} . \tag{9}$$

3. The couette disperser with a single-rotor diameter and four organic liquids [TCE, 2EH, Varsol (hydrocarbon), and a silicone oil] gave

$$\frac{d}{D} = 150(\mathrm{We})^{-0.65}(\mathrm{Re})^{-0.2}\left(\frac{\mu_d}{\mu_c}\right)^{0.5}\left(\frac{D}{ID}\right)^{0.5} . \tag{10}$$

These empirical correlations in the form of Eq. (7) were used for the preparation of nuclear fuel spheres. The effects on d of changes in disperser diameters, flow rates, or couette disperser rotational speed were easily and dependably predicted by the correlations.

For operation with a new pair of process fluids, it was usually more convenient to determine the effect of the fluid properties from a brief period of test operation instead of waiting for laboratory measurements. The drop diameter of the test batch was measured, and the disperser flow rate or rpm was changed according to the empirical correlation to adjust the drop diameter as desired.

Several comparisons can be made concerning the consistency of the empirical correlations. The calculated values of d are listed for comparison with the experimental values (Tables 1 through 5). The relationship of d proportional to $V^{-1.5}$ can be easily checked for many different sets of literature data. While correlations of d with $\mathrm{We}^{-0.6}$ are commonly suggested (based on the theory of turbulent dispersion), much of the data show better agreement with d proportional to $V^{-1.5}$. The data of Middleman[11] for benzene in water covers a wide range of We and is shown on Fig. 5. The data of Karabelas[12] for tubes shows better agreement with d proportional to $V^{-1.5}$ than with $V^{-1.2}$. For another comparison, look at the constants, C_1, for the three types of dispersers. In the static mixers, the hydraulic diameter is perhaps 0.3 ID, and the velocity is doubled as a result of the reduced cross sections and the longer flow path. In the couette disperser, the true average fluid velocity is less than half the rotor velocity, and the D/ID term also is significant. In both cases, a large part of the difference in constants is accounted for. However, the static mixer gives smaller drops and the couette disperser gives larger drops than the tube at comparable We, Re, and D values.

Table 1. Simple tube or turbulent two-fluid nozzle for internal gelation of UO_3

Organic and properties	Organic viscosity (μ_c, cP)	D (cm)	F+G (cm^3/min)	We	Re	Mean drop diameter, d (μm) Experimental	Calculated[a]	P (10^6 cm^2/s^3)	$C_2\,d/d_{max}$ (dimensionless)
TCE	0.40	0.16	515	1916	23,600	75	91	6.32	0.770
ρ = 1.38	0.40		430	1335	19,700	100	120	3.84	0.840
γ = 21 dynes/cm	0.42		390	1099	17,000	120	136	2.95	0.907
(0.021 N/m)	0.36		375	1016	19,100	100	152	2.56	0.714
	0.43		350	885	14,900	130	159	2.20	0.873
	0.40		350	885	16,000	160	163	2.16	1.069
	0.37	0.32	1210	1322	29,900	190	230	0.593	0.756
	0.40		1120	1133	25,600	200	252	0.500	0.744
	0.40		920	764	21,100	350	340	0.292	1.049
	0.48		510	235	9700	636	780	0.0603	1.011
	0.48		510	235	9700	636	780	0.0598	1.011
2EH	2.2	0.16	450	1759	2140	70	67	5.84	0.776
ρ = 0.79	2.4		440	1681	1920	70	67	5.05	0.732
γ = 10 dynes/cm	2.4		430	1606	1880	70	69	4.79	0.717
(0.01 N/m)	1.4		395	1355	2960	75	93	3.93	0.710
	1.3		350	1064	2820	90	113	3.02	0.766
	2.2		340	1004	1490	110	101	2.52	0.872
	2.2		330	946	1570	120	106	2.59	0.963
	2.2		320	889	1530	130	110	2.44	1.016
	2.4		300	782	1310	112	119	2.35	0.863
	2.8		295	756	1100	111	117	2.67	0.899
	2.4		290	730	1270	128	125	2.18	0.956
	2.4		270	633	1180	120	139	1.77	0.825
	2.4		265	610	1160	145	143	1.84	1.011
	1.6	0.32	1320	1891	4320	110	129	1.26	0.662
	1.3		1220	1616	4920	120	155	0.962	0.646
	2.0		965	1010	2530	220	193	0.450	0.874
	1.8		705	540	2050	250	319	0.175	0.682
iAA	0.8	0.32	660	4324	2364	100	158	0.144	0.663
ρ = 0.79									
γ = 2 dynes/cm									
(0.002 N/m)									

[a]
$$\frac{d}{D} = 15(We)^{-0.65}(Re)^{-0.2}\left(\frac{\mu_d}{\mu_c}\right)^{0.5} = 15\left[\frac{D\rho}{\gamma}\left(\frac{F+G}{15\pi D^2}\right)^2\right]^{-0.65}\left[\frac{D\rho}{\mu_c}\,\frac{F+G}{15\pi D^2}\right]^{-0.2}\left(\frac{\mu_d}{\mu_c}\right)^{0.5},$$

$\mu_d = 6\,cP\ (6\,mPa{\cdot}s)$.

Table 2. Simple tube or turbulent two-fluid nozzle for gelation by extraction of water

Organic and properties	Organic viscosity (μ_c, cP)	D (cm)	F+G (cm^3/min)	We	Re	Mean drop diameter, d (μm) Experimental	Calculated[a]	P (10^6 cm^2/s^3)	C_2 d/d_{max} (dimensionless)
iAA	2.5	0.15	530	5600	2400	25	21	15.00	0.618
ρ = 0.80	2.0	0.195	870	7350	3790	20	24	12.01	0.452
γ = 5 dynes/cm	2.8	0.20	440	1740	1335	95	66	1.517	0.939
(0.005 N/m)	2.3		415	1550	1530	75	77	1.107	0.653
	2.2		395	1410	1525	80	84	0.972	0.662
	2.3		220	436	812	170	199	0.316	0.896
	2.7	0.265	655	1660	1555	127	90	0.603	0.868
	2.7		560	1210	1330	145	113	0.437	0.871
	2.7		545	1150	1295	145	118	0.420	0.858
	2.7	0.280	510	854	1145	180	155	0.263	0.882
	3.1	0.380	1065	1490	1535	140	129	0.208	0.625
	3.1		965	1220	1390	175	150	0.173	0.726
	2.9		750	738	1155	265	223	0.0967	0.871
	3.0		720	681	1070	280	235	0.0934	0.907
	2.5	0.40	890	892	1510	175	212	0.0871	0.551
	2.9	0.49	1300	1035	1555	175	218	0.0639	0.487
	2.9	0.50	1300	974	1525	190	232	0.0559	0.501
2EH	5.1	0.195	625	1050	1067	165	110[a]	6.54	1.356
ρ = 0.80	5.7		525	744	802	185	138[a]	5.16	1.383
γ = 18 dynes/cm	5.0		335	303	584	230	179	1.84	1.138
(0.018 N/m)	3.5	0.200	380	361	922	300	282[b]	1.43	1.344
	4.8		250	156	442	300	303	0.852	1.091

[a]
$$\frac{d}{D} = 15(We)^{-0.65}(Re)^{-0.2}\left(\frac{\mu_d}{\mu_c}\right)^{0.5} = 15\left[\frac{D\rho}{\gamma}\left(\frac{F+G}{15\pi D^2}\right)^2\right]^{-0.65}\left[\frac{D\rho}{\mu_c}\,\frac{F+G}{15\pi D^2}\right]^{-0.2}\left(\frac{\mu_d}{\mu_c}\right)^{0.5},$$

$\mu_d = 4\ cP\ (4\ mPa{\cdot}s)\ (ThO_2\ sol)$.

[b] UO_2 sol, estimated μ_d = 10 cP (10 mPa·s).

Table 3. Static (Kenics) mixers for internal gelation of UO_3

Organic and properties	ID (cm)	F+G (cm^3/min)	We[a]	Re[a]	Mean drop diameter, d (μm) Experimental	Calculated[b]	P (10^6 cm^2/s^3)	C_2 d/d_{max} (dimensionless)
2EH	0.335[e]	500	236	1043	40	45	4.441	0.401
ρ = 0.79		340	109	709	112	81	2.027	0.820
γ = 10 dynes/cm		300	85	626	110	98	1.578	0.745
(0.010 N/m)		300	85	626	112	98	1.578	0.759
μ_c = 2 cP (2 mPa·s)		290	80	605	128	103	1.481	0.827
		270	69	563	120	114	1.285	0.732
		240	54.5	501	155	136	1.014	0.860
	0.493[c]	345	35.3	489	250	267	0.203	0.729
		345	35.3	489	291	267	0.203	0.849
		345	35.3	489	280	267	0.203	0.816
		130	5.0	184	500	1155[d]	0.029	0.670
TCE	0.493[b]	310	55.4	4090	296	301	0.0269	0.569
ρ = 1.38		310	55.4	4090	280	301	0.0296	0.538
γ = 9 dynes/cm[e]		275	43.6	3630	310	361	0.0193	0.521
μ_c = 0.45 cP (0.45 mPa·s)	0.794[c]	986	134	8090	250	238	0.0262	0.475
		787	85.4	6450	290	334	0.0141	0.430
		767	81.1	6290	300	347	0.0132	0.433
		747	77.0	6130	300	361	0.0122	0.419
		717	70.9	5880	309	384	0.0109	0.413
		717	81.1	5880	305	384	0.0109	0.408
		552	42.0	4530	600	569	0.0053	0.602
		507	35.5	4160	640	646	0.0042	0.584
		507	35.5	4160	610	646	0.0042	0.557
		507	35.5	4160	620	646	0.0042	0.566

[a]We and Re values are calculated using an ID instead of a hydraulic diameter.

[b]
$$\frac{d}{D} = 1.2(We)^{-0.65}(Re)^{-0.2}\left(\frac{\mu_d}{\mu_c}\right)^{0.5} = 1.2\left[\frac{ID\rho}{\gamma}\left(\frac{F+G}{15\pi D^2}\right)^2\right]^{-0.65}\left[\frac{ID\rho}{\mu_c}\,\frac{F+G}{15\pi ID^2}\right]^{-0.2}\left(\frac{\mu_d}{\mu_c}\right)^{0.5},$$

$\mu_d = 6\,cP\,(6\,mPa{\cdot}s)$.

[c]Kenics Corporation, North Andover, Mass., model numbers 37-03-062 for 0.335 cm ID, 37-04-065 for 0.493 cm ID, and 37-06-109 for 0.794 cm ID; 21 elements in each unit.

[d]The turbulent shear correlation is probably not valid because of the low flow rate and low Reynolds number.

[e]Low interfacial tension after long-term recycle of TCE and an accumulation of organic solutes.

Table 4. Couette or annular disperser for internal gelation of UO_3

Organic liquid and properties	D, or 1/2 annulus thickness (cm)	Rotor (rpm)	We	Re[a]	Mean drop diameter, d (μ) Experimental	Calculated[b]	P (10^6 cm^2/s^3)	C_2 d/d_{max} (dimensionless)
TCE	0.316	1350	1062	11,000	822	913	0.036	1.066
ρ = 1.38		1800	1888	14,600	594	593	0.079	1.055
γ = 21 dynes/cm		2400	3360	19,500	429	385	0.172	1.040
(0.021 N/m)		2400	3360	19,500	429	385	0.172	1.040
μ_o = 0.45 cP		3200	5790	26,000	218	250	0.383	0.835
(0.45 mPa·s)	0.504	2400	5350	31,100	448	522	0.097	0.926
		3200	9520	41,400	302	339	0.213	0.798
2EH	0.316	1200	1010	900	451	624	0.057	0.785
ρ = 0.79		1800	2270	1340	214	340	0.130	0.518
γ = 10 dynes/cm		2400	4040	1790	107	220	0.229	0.325
(0.01 N/m)	0.504	1200	1610	1430	670	845	0.0226	0.806
μ_o = 2.8 cP								
(2.8 mPa·s)								
Varsol	0.316	1800	629	2570	828	1010	0.109	0.865
ρ = 0.70		2460	1170	3510	774	632	0.276	1.172
γ = 34 dynes/cm		3160	1940	4500	333	434	0.574	0.676
(0.032 N/m)	0.504	2400	1782	5460	783	889	0.150	0.929
μ = 1.3 cP								
(1.3 mPa·s)								
Silicone oil	0.316	1200	367	58	408	492	0.886	1.160
ρ = 0.92		1800	826	88	299	268	1.983	1.174
γ = 32 dynes/cm		1800	826	88	347	268	1.983	1.362
(0.032 N/m)	0.514	2400	1470	117	190	174	3.520	0.938
μ_o = 50 cP		1200	586	93	500	667	0.346	0.977
(50 mPa·s)		1200	586	66[c]	409	603[a]	0.484	0.914
		1800	1320	156[d]	323	374[d]	0.702	0.837
TCE	0.316	2400	7830	19,500	290	222	0.172	1.170
ρ_o = 1.38		2400	7830	19,500	280	222	0.172	0.129
γ = 9 dynes/cm[e]		2800	10,700	22,700	230	176	0.265	1.102
(0.009 N/m)								
μ_o = 0.45 cP								
(0.45 mPa·s)								

[a]Re number based on average liquid velocity = 0.5 × rotor velocity.

[b]

$$\frac{d}{D} = 150(We)^{-0.65}(Re)^{-0.2}\left[\frac{\mu_d}{\mu_c}\right]^{0.5}\left[\frac{D}{ID}\right]^{0.5}$$

$$\frac{d}{D} = 150\left[\frac{D\rho}{\gamma}\left[\frac{rpm\,\pi ID}{60}\right]^2\right]^{-0.65}\left[\frac{D\rho}{\mu_c}\,\frac{rpm\,\pi ID}{120}\right]^{-0.2}\left[\frac{\mu_d}{\mu_c}\right]^{0.5}\left[\frac{D}{ID}\right]^{0.5},$$

$\mu_d = 6\,cP\,(6\,mPa{\cdot}s)$,

Rotor diameter, ID = 3.2 cm .

[c]Lower silicone oil temperature; thus μ = 70 cP.

[d]Higher silicone oil temperature; thus μ = 45 cP.

[e]Low interfacial tension after long-term recycle of TCE and an accumulation of organic solutes.

Table 5. Couette or annular disperser (tapered annulus) for internal gelation of UO_3

Organic liquid and properties	D, or 1/2 annulus thickness (cm)	Rotor (rpm)	We	Re[a]	Mean drop diameter, d (μ) Experimental	Mean drop diameter, d (μ) Calculated[b]	P (10^6 cm^2/s^3)	C_2 d/d_{max} (dimensionless)
TCE	0.316	1800	1340	12,300	940	833	0.051	1.401
ρ = 1.38		2400	2390	16,400	640	541	0.108	1.289
γ = 21 dynes/cm		2400	2390	16,400	628	541	0.108	1.264
(0.021 N/s)		3000	3730	20,500	397	387	0.202	1.027
μ_o = 0.45 cP		3200	4350	21,900	355	351	0.241	0.985
(0.45 mPa·s)		3750	5840	25,700	241	277	0.371	0.795
	0.476	1800	2025	18,600	1331	1087	0.0235	1.456
		2400	3600	24,800	901	706	0.052	1.354
		3180	6320	32,800	409	463	0.110	0.830
		3180	6320	32,800	392	463	0.110	0.830
	0.676	1800	2880	26,400	1455	1366	0.0117	1.204
		2400	5110	35,200	992	886	0.026	1.130
		2400	5110	35,200	1104	886	0.026	1.258
		3180	8977	46,600	528	582	0.056	0.817

[a]Based on average liquid velocity of 0.5 × rotor velocity.

[b]
$$\frac{d}{D} = 150(We)^{-0.65}(Re)^{-0.2}\left(\frac{\mu_d}{\mu_c}\right)^{0.5}\left(\frac{D}{ID}\right)^{0.5} ,$$

$$\frac{d}{D} = 150\left[\frac{D\rho}{\gamma}\left(\frac{rpm\,\pi ID}{60}\right)^2\right]^{-0.65}\left[\frac{D\rho}{\mu_c}\,\frac{rpm\,\pi ID}{120}\right]^{-0.2}\left(\frac{\mu_d}{\mu_c}\right)^{0.5}\left(\frac{D}{ID}\right)^{0.5} ,$$

$\mu_d = 6\,cP\,(6\,mPa{\cdot}s)$,

Rotor diameter, ID = 2.7 cm (estimated effective).

5. CORRELATION OF RESULTS BY TURBULENT DISPERSION THEORY

The basic theory of turbulent dispersion indicates that the drop sizes should follow the relationship, as previously presented in Eq. (1),

$$d_{\max} = C_2 \left[\frac{\gamma}{\rho}\right]^{0.6} P^{-0.4} .$$

The gel-sphere results for turbulent dispersion were primarily concerned with control of the average diameter, d, by control of the flow rate or the couette disperser rpm. A typical set of experimental data is the dimensions of the disperser, the flow rate or the couette disperser rpm, the average diameter of the product, the shrinkage factor, SF, for drop and product diameter, and periodic measurements of fluid properties for samples of the process fluids. With some reasonable calculations, the gel-sphere results can be shown to agree with turbulent dispersion theory.

The discussions of and selection of values of $d_{\max}$ from size distribution measurements are somewhat ambiguous and uncertain. Many authors suggest use of d_{95} as $d_{\max}$ while others attempt to identify the largest drop of a sample. The gel-sphere data will first be examined by rearranging Eq. (1) as follows:

$$C_2 \left[\frac{d}{d_{\max}}\right] = P^{0.4} d \left[\frac{\gamma}{\rho}\right]^{-0.6} . \tag{11}$$

The measured size distribution of gel-sphere products from turbulent dispersion showed

$$\frac{d}{d_{95}} \text{ of } 0.52 \text{ to } 0.67 ,$$

$$\frac{d}{d_{98}} \text{ of } 0.43 \text{ to } 0.60 .$$

Therefore $d_{\max}/d = 1.8$ is used to allow comparisons of the gel-sphere data with theory.

The concentrations and densities of the aqueous feeds were determined for every test, as these values were necessary to calculate shrinkage ratios. The densities and viscosities of the organic liquids were handbook values with corrections for the measured temperatures. The interfacial tensions and the viscosities of the aqueous feeds were measured periodically on samples taken from the process but were not measured for every gel-sphere test. These measured interfacial tensions were static or equilibrium values for the process fluids. For

the internal type of gelation, the interfacial tensions were measured separately for the organic samples versus the two stable aqueous solutions, as the mixed solutions thicken too rapidly at room temperature for convenient measurement. The two stable solutions gave approximately the same values of interfacial tensions.

Even though the interfacial tensions were measured for samples of the process fluids, the results have the following serious uncertainties:

1. The process organics all contained a sorbitan mono-oleate surfactant (usually 0.1 to 1 vol % for drop formation by turbulent mechanisms). The new surface formed during turbulent dispersion requires a finite time to approach the equilibrium surface tensions measured in the laboratory.
2. For the gelation-by-water extraction, the water concentrations near the interface would be different for the lab measurements and the turbulent dispersion.
3. For the internal type of gelation, the laboratory measurements are for two separate concentrated solutions at temperature equilibrium while the turbulent dispersion during process operation involves the mixed aqueous solution starting at 0°C and the organic liquid at 60 to 90°C.

Because of these uncertainties, the exponents for Weber and Reynolds numbers in the empirical correlations were evaluated for sets of data with the disperser dimensions and the flow rates as variables and the fluid properties constant. The fluid properties were then used to evaluate the remaining constants in the empirical correlations. The results indicate that any bias in the measurement of interfacial tensions is uniform or consistent, as the empirical constants did not differ significantly for the different organic liquids.

All power inputs were calculated from the disperser dimensions and flow rates or rpm. The basic form of equation for calculating frictional pressure drops by using a Fanning friction factor[13] is

$$\frac{\Delta P}{L} = 2\frac{fV^2}{D} = \frac{32fQ^2}{\pi^2 D^5} \quad . \tag{12}$$

$f = 16/\mathrm{Re}$ for $\mathrm{Re}<2000$,

$f = 0.08/\mathrm{Re}^{0.25}$ for $\mathrm{Re}>4000$,

$f = 0.10$ for Re 2000 to 4000.

Multiplication by the velocity gives a power per unit mass as follows:

$$P = \frac{\Delta PV}{L} = 2\frac{fV^3}{D} = \frac{128fQ^3}{\pi^3 D^7} \quad . \tag{13}$$

Substitution of $f = 16/\mathrm{Re}$ for laminar flow conditions gives:

$$P = \frac{\Delta PV}{L} = \frac{32\mu V^2}{D^2\rho} = \frac{512\,\mu Q^2}{\pi^2\rho D^6} \quad . \tag{14}$$

Substitution of $f = 0.08/\mathrm{Re}^{0.25}$ for turbulent flow conditions gives

$$P = \frac{\Delta PV}{L} = \frac{0.16\mu^{0.25}V^{2.75}}{D^{1.25}\rho^{0.25}} = \frac{2.56\mu^{0.25}Q^{2.75}}{\pi^{2.75}\rho^{0.25}D^{6.75}} \quad . \tag{15}$$

For the couette disperser, the basic definition of viscosity gives the following expressions for laminar flow (annulus thickness $= D/2$):

$$\text{Force} = \frac{2\mu VA}{D} \quad . \tag{16}$$

$$P = \left(\frac{2\mu AV}{D}\right)\left(V\right)\left(\frac{2}{DA\rho}\right) = \frac{4\mu}{D^2\rho}V^2 \quad . \tag{17}$$

Note that the fluid velocity will only average half of the rotor velocity so that

$$\mathrm{Re} = \frac{D\rho V}{2\mu} \quad . \tag{18}$$

For laminar flow with $f = 16/\mathrm{Re}$ and by comparison of Eq. (17) with Eq. (13) and (14),

$$P = \frac{4\mu V^2}{D^2\rho} = \frac{1}{8}\frac{fV^3}{D} \quad . \tag{19}$$

For turbulent flow, use $f = 0.08/\mathrm{Re}^{0.25}$ to give

$$P = 0.01189\,\frac{\mu^{0.25}V^{2.75}}{\rho^{0.25}D^{1.25}} \quad , \tag{20}$$

The manufacturer's literature for the Kenic static mixers gives pressure-drop equations as

$$\text{Pressure drop (psi)} = [\text{flow rate (gpm)}] \times [\text{viscosity(cps)}] \times [\mathrm{A}'] \quad . \tag{21}$$

The values of A' are 2.1, 0.55, and 0.13 for the three static mixers used in this study. This equation has the form of a laminar flow equation. By setting Eq. (21) equal to the laminar flow equation for pressure drop, values of D can be calculated and are 0.62 ID to 0.64 ID. Use of the experimentally measured void volumes and some assumptions for velocities and hydraulic diameters also indicates that $D \simeq 0.6$ ID. Therefore, 0.62 ID was used as the value of D to calculate values of P for the Kenic mixers.

The values of energy dissipation per unit mass of liquid were calculated using these equations and assumptions (Tables 1 through 5). Values of $C_2(d/d_{\max})$ from Eq. (11) are also in these tables. The average of 48 values of $C_2(d/d_{\max})$ with Re >2000 for Tables 1 through 4 is 0.769. For $d/d_{\max} = 1.8$, this gives an average value of 1.38 for C_2. During turbulent dispersion with formation of new interfacial area, the true values of the interfacial tensions are probably higher than the measured equilibrium values used for calcula-

tions. Use of higher values of γ in Eq. (11) would give smaller values of C_2. The maximum reasonable values of γ would be those for pure liquids, and the high sorbitan monooleate concentrations in the organic liquid probably result in a rapid approach to equilibrium interfacial tensions. The values of C_2 for Re <2000 average only 13% higher than the values for Re >2000.

The agreement of the gel-sphere data with turbulent dispersion theory is shown by plotting P versus 1.8 $d\ (\gamma/\rho)^{-0.6}$ (Fig. 6). For the couette disperser and the static mixer, only the data for Re >2000 are shown. For the tube disperser, data for Re for 1100 to 2000 are shown with a separate symbol for comparison. Figure 6 also shows the values found by Davies[3] for four emulsifying machines. A line is shown for Eq. (1) with C_2 = 1.2. This figure shows that Eq. (1) with a constant in agreement with theory can be applied for a wide (10^9) range of energy dissipation rates, P for Re >2000. For Re <1000, the drop sizes were larger but were within a factor of 2 of the values predicted by Eq. (1). As mentioned previously, if the true interfacial tensions were between those from equilibrium measurements and those for pure liquids, the values of C_2 would be smaller and closer to the theoretical value for turbulent dispersion. Using C_2 = 1.2 and d_{max} = 1.8, the gel-sphere results can be represented by

$$d = \frac{2}{3}\left(\frac{\gamma}{\rho}\right)^{0.6} P^{-0.4} \ . \tag{22}$$

Since Eqs. (15) and (20) give P proportional to $V^{2.75}$, then d_{max} from Eq. (1) should be proportional to $V^{-1.10}$. But the data and literature data for single dispersers and fluid pairs show d proportional to $V^{-1.5}$. Some (but not all) of the dependencies on $V^{-1.5}$ are explained by the indeterminate friction factors in the transition region for Re <4000.

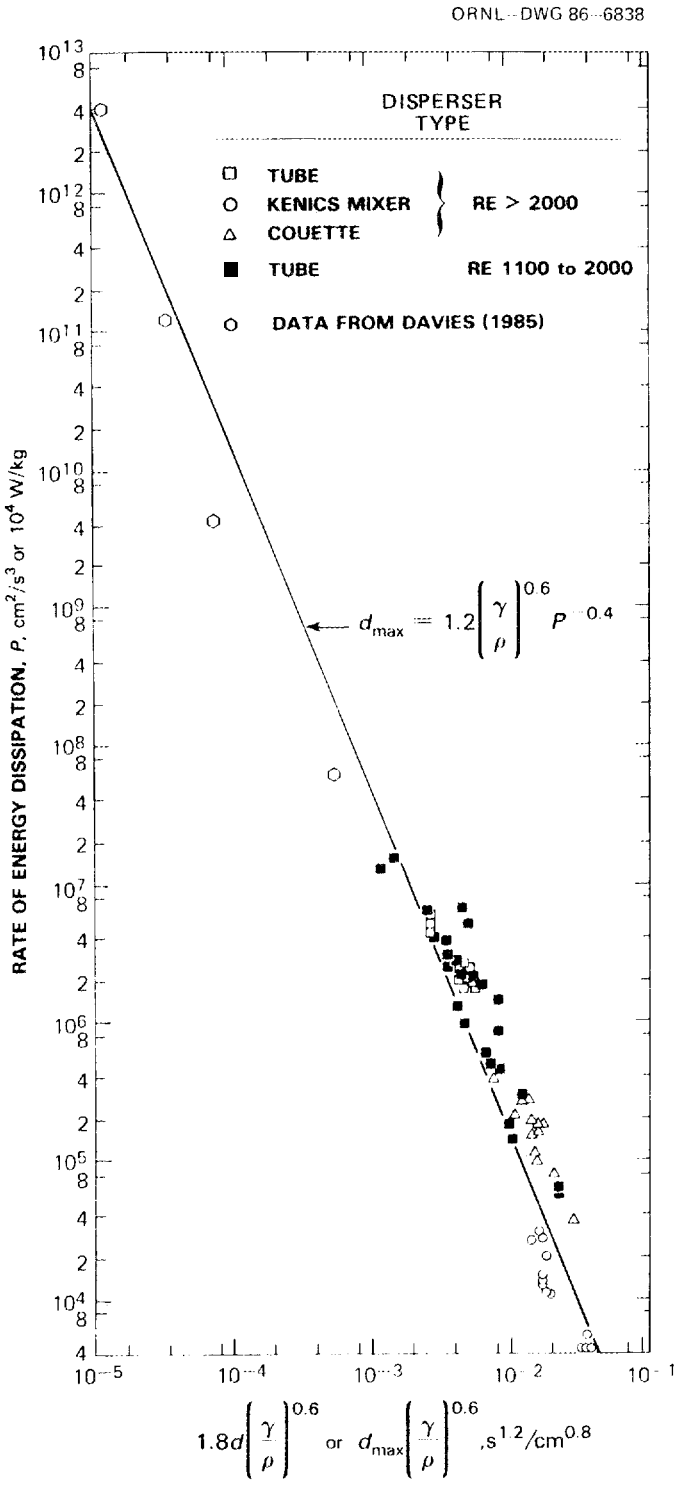

Fig. 6. Experimental data for turbulent dispersion.

6. COMPARISONS OF CORRELATIONS WITH LITERATURE DATA

Some of the turbulent dispersion data in the literature is of interest for examining the effects of individual variables. Such selected comparisons are discussed here. The data of Karabelas[12] is for dispersion of water into two hydrocarbons with viscosities that differed by a factor of 10. The empirical form of correlation using $(\mu_d/\mu_c)^{0.5}$ accounts very well for the viscosity effect (Table 6). But the empirical constant is 50 as compared to the gel-sphere constant of 15 for tubes of much smaller diameter. The plot of $1.8\ d\ (\gamma/\rho)^{-0.6}$ versus calculated values of P shows only a fair agreement with Eq. (1) for kerosene as the continuous phase, but the agreement is distinctly poorer for the viscous transformer oil as the continuous phase (Fig. 7). The viscous force term suggested by Davies[3] (Eq. 2) is for the discontinuous phase and does not account for the viscosity effect.

The data of Middleman[11] describe Kenics mixers using water as the continuous phase. The data for dispersion of benzene are for a wide range of Weber numbers. The average drop diameter versus $We^{0.5}$ has a slope of -1.5 for most of this range (Fig. 5), and this agrees with the d versus velocity or speed dependence for the gel-sphere data. Middleman gives a friction factor of 100 times the factor for a tube. For a void volume of two-thirds of the open tube volume (this may be low for the larger Kenics mixers), the values of P would be 150 times those from Eq. (13). These values of P give an excellent agreement with the theoretical correlation for turbulent dispersion (Fig. 7). However, the values of P are higher than would be expected from scale-up of the pressure drop equations for the smaller Kenics mixers.

Table 6. Simple tube dispersion data of Karabelas (1978)

Organic and properties	Velocity, V (cm/s)	We	Re	Mean drop diameter, d (μm) Experimental	Mean drop diameter, d (μm) Calculated[a]	P (10^6 cm^2/s^3)	$C_2\, d/d_{max}$ dimensionless
Kerosene	298	9490	75,100	416	563	0.0510	0.314
ρ = 0.7	257	7061	64,800	479	702	0.0338	0.308
γ = 33 dynes/cm (0.033 N/m)	222	5270	55,900	828	875	0.0226	0.453
μ_c = 1.4 cP (1.4 mPa·s)	184	3620	46,400	1108	1159	0.0134	0.492
	152	2470	38,300	2133	1544	0.0079	0.769
	152	2470	38,300	1743	1544	0.0079	0.628
	118	1490	29,700	1960	2258	0.0040	0.536
Transformer oil	300	9070	7560	345	290	0.0920	0.319
ρ = 0.70	260	6810	6550	397	359	0.0614	0.312
γ = 35 dynes/cm (0.035 N/m)	224	5060	5640	520	449	0.0410	0.348
μ_c = 14 cP (14 mPa·s)	208	4360	5240	426	502	0.0336	0.269
	186	3490	4690	710	594	0.0245	0.387
	152	2330	3830	916	804	0.0137	0.395
	119	1430	3000	804	1161	0.0070	0.266

[a]

$$\frac{d}{D} = 50(We)^{-0.65}(Re)^{-0.2}\left(\frac{\mu_d}{\mu_c}\right)^{0.5},$$

D = 5.04 cm,
μ_d = 1.0 cP.

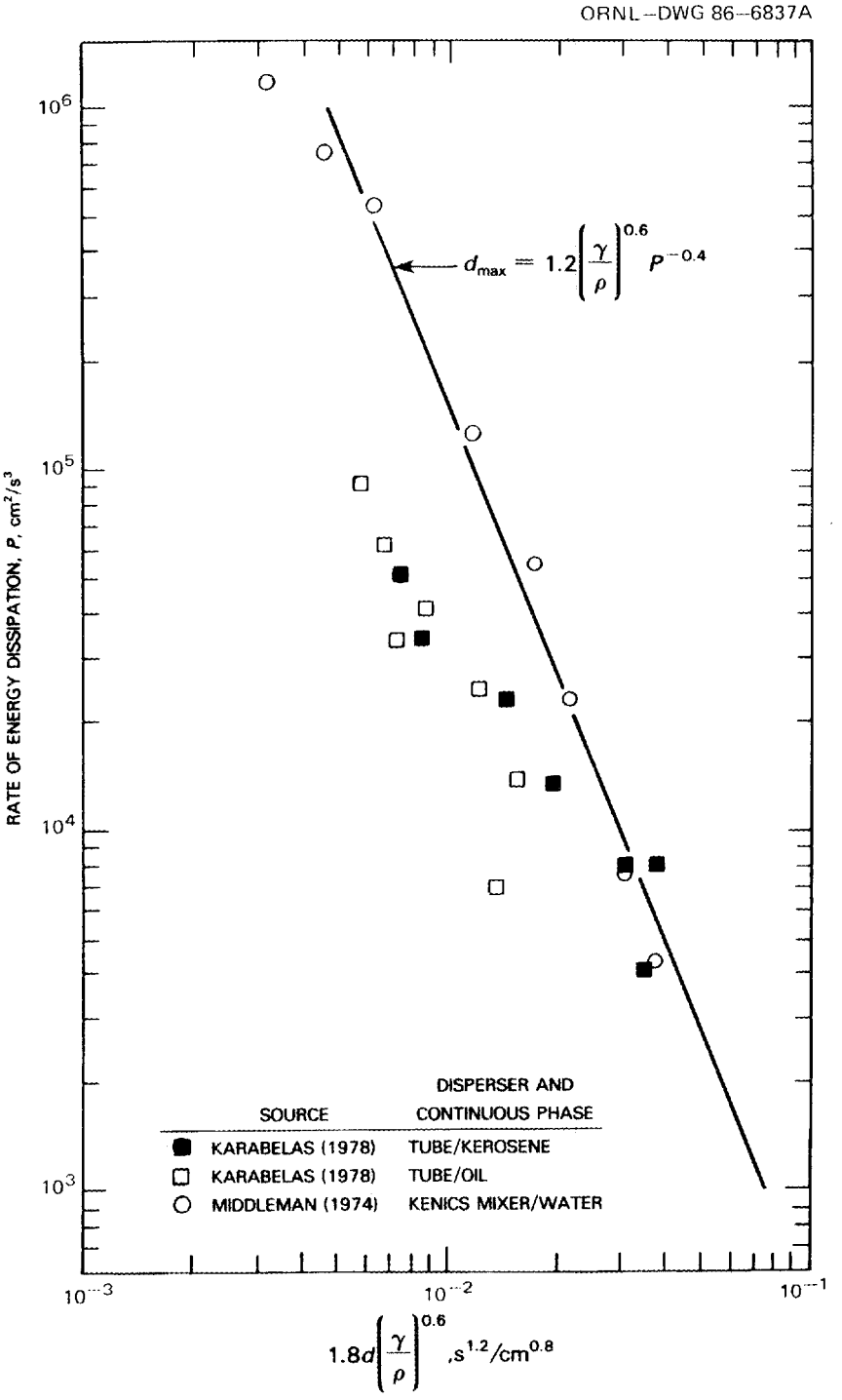

Fig. 7. Correlation of selected literature data by turbulent dispersion theory.

7. APPLICATION TO ANNULAR MIXING FOR CENTRIFUGAL CONTACTORS

An advanced design of centrifugal contactors has been proposed and developed for solvent extraction for reprocessing of nuclear fuels. The dispersion and coalescence for turbulent couette flow in these contactors has been studied by Leonard[14]. A spinning rotor provides dispersion and mixing by turbulent couette flow in an annulus between the rotor and a stationary housing and provides a centrifugal separation of the two phases within the rotor. The rotor and the housing are designed to act as a pump for liquid transfer. The rotor dimensions and speed are selected to meet the separation requirements for the solvent extraction process. The housing configuration is partly determined by the requirements for pumping, and the design variables applicable to meeting the mixing requirements are limited. Fortunately, the annular mixing gives good dispersion and good mixing, and high stage efficiencies are usually achieved without difficulty. As a result, the dispersion in these annular mixers has received little study. The annular mixing for these centrifugal contactors is very similar to the annular or couette dispersion for the gel-sphere processes. Therefore, the same turbulent dispersion theory and calculations should apply to both.

A calculation of Reynolds numbers using Eq. (18) for the annulus will indicate whether turbulent dispersion will occur. The hydraulic diameter for a thin annulus is twice the annulus thickness. The density and viscosity for organic continuous operation in a nuclear fuel reprocessing plant might be 0.8 g/cm^3 or higher (30% TBP in a hydrocarbon diluent) and 1.5 centipoise. The average liquid velocity will be one-half of the rotor speed as the liquid is bounded by the rotor on one side of the annulus and a stationary housing on the other side. The typical design and operating values for a large and a small centrifugal contactor give the following:

25-cm contactor, 1200 rpm, $D = 2(2.35) = 4.70$ cm;

$$\mathrm{Re} = \frac{(4.70)(1200)(\pi)(26.5)(0.8)}{(60)(2)(0.015)} = 208{,}000.$$

5.5-cm contactor, 4000 rpm, $D = 2(0.64) = 1.28$;

$$\mathrm{Re} = \frac{(1.28)(4000)(\pi)(5.5)(0.8)}{(60)(2)(0.015)} = 39{,}000.$$

It appears that turbulent dispersion will take place for all likely operating conditions.

The rates of energy dissipation in the annular mixing zone can be calculated using Eq. (20) for turbulent flow and $f = 0.08/\mathrm{Re}^{0.25}$;

$$P = \frac{0.01189\mu^{0.25}V^{2.75}}{(D)^{1.25}\rho^{0.25}}$$

Calculations for the 25-cm centrifugal contactor include

$$V = \frac{\pi D\ rpm}{60} = \frac{(\pi)(26.5)(1200)}{60} = 1665\ \mathrm{cm/s}\ ,$$

$$P = \frac{(0.00375)(1665)^3}{(8)(4.70)} = 460{,}000\ \mathrm{cm^2/s^3}\ .$$

Calculations for the 5.5-cm centrifugal contactor include

$$V = \frac{\pi D\ rpm}{60} = \frac{(\pi)(5.5)(4000)}{60} = 1152\ \mathrm{cm/s}\ ,$$

$$P = \frac{(0.0057)(1152)^3}{(8)(1.28)} = 851{,}000\ \mathrm{cm^2/s^3}\ .$$

The lowest operating speeds will be about half of these values to give about one-seventh of the above values of P. Using Eq. (22) and values of $\rho = 0.8\ \mathrm{g/cm^3}$ and $\gamma = 8$ dyn/cm, the calculated average drop diameters are

$$d = \frac{2}{3}\left[\frac{\gamma}{\rho}\right]^{0.6}(P)^{-0.4}\ .$$

For the largest P of $0.85 \times 10^6\ \mathrm{cm^2/s^3}$,

$$d = 0.0113\ \mathrm{cm\ or\ 113\ \mu m}.$$

For the smallest P of $0.066 \times 10^6\ \mathrm{cm^2/s^3}$,

$$d = 0.031\ \mathrm{cm\ or\ 310\ \mu m}\ .$$

For a log-normal distribution with a typical γ for the couette disperser, about 1 wt % of the drops would be smaller than 0.4 d.

The procedure used to calculate the energy dissipation for couette dispersion will give the mixing power for annular mixing. The weight of liquid in an annular mixing zone is π $(D/2)$, (H) $(\mathrm{ID})\rho$, where H is the height of the zone. The total mixing power, TMP, is P times this amount or

$$\mathrm{TMP} = 0.5\ \pi DH(\mathrm{ID})\rho P = (\pi/2)\ (D)\ (H)(\mathrm{ID})\rho\ \mathrm{f}V^3/8D.$$

For the 25-cm contactor,

$$\mathrm{TMP} = 71.9\ 10^6 H\ \mathrm{g \cdot cm^2/s}$$

For $H = 10$, TMP = 71.9 W.

For the 5.5-cm contactor and $H = 3$ at 4000 rpm,

$$\mathrm{TMP} = 2.3\ \mathrm{W}.$$

The total power required for a centrifugal contactor will also include the pumping power, the energy loss below the rotor, and the power required to accelerate liquids in the rotor.

8. RESULTS AND CONCLUSIONS

Drop sizes for turbulent dispersion of aqueous solutions in organic liquids were determined for three types of dispersion devices, which were selected to give nearly homogeneous and isotropic turbulence. The gel-sphere processes as used for preparation of nuclear fuels provided a convenient and reproducible measurement of the size distribution of product spheres and of the aqueous solution drops in the organic liquids. Uncertainties in the appropriate values of the interfacial tensions for gel-sphere process conditions are a major problem for correlation of results.

Empirical correlations of average drop diameters were determined using the results of a dimensional analyses and assuming an exponential form. The exponents for Weber and Reynolds numbers in the empirical correlations were evaluated without the use of interfacial tension values. Laboratory equilibrium values for interfacial tensions were measured using samples of process fluids, and these values were used to determine the remaining empirical constants. These empirical correlations are convenient for selection of gel-sphere preparation conditions but should not be extrapolated.

A theory of turbulent dispersion involving eddy velocities and the rate of energy dissipation provides a theoretical correlation for maximum drop diameters. The theory of homogeneous, isotropic turbulence was originated by Kolmogoroff[1]. Davies[3] compares this theory with four types of dispersion devices with high rates of energy dissipation. The gel-sphere data were compared in the same way using calculated values of the rate of energy dissipation, P, and using $d_{\max} = 1.8\ d$, where d is the weight average diameter, and d_{max} is the maximum diameter of the turbulent dispersion theory. The gel-sphere results show good agreement with Eq. (22).

$$d = \frac{2}{3}\left(\frac{\gamma}{\rho}\right)^{0.6} P^{-0.4} ,$$

where γ is the interfacial tension measured for process samples and ρ is the continuous phase density. The range of values for P was 10^3 to 10^7 cm^2/s^3 or 10^{-1} to 10^3 W/kg. Using $d_{\max} = 1.8\ d$, the values of Davies[3] and the gel-sphere results together show agreement with the turbulent dispersion theory for P of 10^3 to 4×10^{12} cm^2/s^3. The relationship is

$$d_{\max} = 1.2\left(\frac{\gamma}{\rho}\right)^{0.6} P^{-0.4} . \tag{23}$$

Application of the turbulent dispersion results to annular mixing for centrifugal contactors as used for reprocessing of nuclear fuels indicates aqueous drop sizes of 110 to 310 μm. The distribution of drop sizes and the mixing power calculations also have applications for centrifugal contactor operation.

REFERENCES

1. A. N. Kolmogoroff, *Dokl. Acad. Nauk, S.S.S.R.* (N.S.) **66**, 825 (1949).

2. J. O. Hinze, "Fundamentals of the Hydrodynamic Mechanism of Splitting in Dispersion Processes," *AIChE J.* **1**(3) 289–95 (1955).

3. J. T. Davies, "Drop Sizes of Emulsions Related to Turbulent Energy Dissipation Rates," *Chem. Eng. Sci.* **40,** 839–42 (1985).

4. P. A. Haas et al., "Preparation of Reactor Fuels by Sol-Gel Processes," *Chem. Eng. Prog. Symp. Ser.* **63**(80), 16–27 (1967).

5. P. A. Haas et al., "Chemical Flowsheet Conditions for Preparing Urania Spheres by Internal Gelation," *Ind. Eng. Chem. Prod. Res. Dev.* **19**, 459–67 (1980).

6. P. A. Haas and S. D. Clinton, "Preparation of Thoria and Mixed-Oxide Microspheres," *Ind. Eng. Chem. Prod. Res. Dev.,* **5**, 236–44 (1966).

7. K. Bischoff et al., "Sol Gel Processes for Carbide Preparation," pp. 95–128 in *Sol-Gel Processes for Fuel Fabrication*, IAEA-161, Vienna (1974).

8. E. Zimmer et al., "Aqueous Chemical Processes for the Preparation of High Temperature Reactor Fuel Kernels," *Radiochim Acta* **25**, 161–69 (1978).

9. P. A. Haas and V. L. Fowler, *Vibration as an Aid to Drop Formation and Application to Gel-Sphere Processes,* ORNL/TM-9091 (June 1984).

10. J. T. Davies, *Turbulence Phenomena*, Academic Press, New York (1972).

11. S. Middleman, "Drop Size Distributions Produced by Turbulent Pipe Flow of Immiscible Fluids Through a Static Mixer," *Ind. Eng. Chem. Process Des. Dev.* **13**(1), 78–83 (1974).

12. A. J. Karabelas, "Drop Size Spectra Generated in Turbulent Pipe Flow of Dilute Liquid-Liquid Suspensions," *AIChE J.* **24** (2), 170–80 (1978).

13. R. H. Perry and C. H. Chilton, *Chemical Engineer's Handbook,* McGraw-Hill, New York (1973).

14. R. A. Leonard et al., "Liquid-Liquid Dispersion in Turbulent Couette Flow," *AIChE J.* **27**(3), 495–503 (1981).

NOMENCLATURE

A	Area of couette flow
A'	Constant in pressure drop correlation for Kenics mixers
a,b,c,g	Exponents for a dimensional analysis correlation
C_1,C_2	Dimensionless constants in correlations of drop diameters
d	Average drop diameter on a volume (or weight) basis
d_{84},d_{95}	Drop diameter with 84 or 95 vol % (or wt %) of the total smaller than d_{84} or d_{95}
d_{max}	Maximum stable drop diameter
D	Hydraulic diameter of dispersion device
$F+G$	Total flow rate of the two phases
f	Fanning friction factor as in Perry[13]
g	Gravitational constant
ID	Other diameter dimension (i.e., inside diameter for static mixer and rotor diameter for couette disperser)
L	Length of flow channel
P	Rate of energy dissipation per unit mass of liquid
ΔP	Pressure drop due to friction
Q	Volumetric rate of flow
rpm	Revolutions per minute for couette disperser rotor
Re	Reynolds number $= DV\rho/\mu$ (or $DV\rho/2\mu$ for couette disperser)
SF	Shrinkage factor or ratio of drop diameter to gel-sphere product diameter
V	Average velocity
v	Turbulent (eddy) velocity
We	Weber number $= DV^2\rho/\gamma$
γ	Interfacial tension

ρ	Fluid density of continuous phase
$\Delta\rho$	Fluid density difference
σ	Standard deviation for drop size distribution (log-normal basis)
μ_c	Fluid viscosity of continuous phase
μ_d	Fluid viscosity of dispersed phase

ORNL/TM-9950
Dist. Category UC-86

INTERNAL DISTRIBUTION

1. J. O. Blomeke
2. W. D. Bond
3. J. T. Bradbury
4–6. W. D. Burch
7. D. A. Costanzo
8. R. M. Counce
9. S. F. DeMuth
10. R. D. Ehrlich
11. M. J. Feldman
12. R. W. Glass
13. W. S. Groenier
14–18. P. A. Haas
19. J. Halperin
20. M. J. Haire
21. R. T. Jubin
22. E. H. Krieg, Jr.
23. R. E. Leuze
24. B. E. Lewis
25. S. A. Meacham
26. D. R. Moser
27. W. W. Pitt
28–30. R. W. Sharpe
31. B. B. Spencer
32. J. G. Stradley
33. T. D. Welch
34. M. E. Whatley
35. O. O. Yarbro
36. H. R. Yook
37–38. Laboratory Records
39. Laboratory Records, ORNL-RC
40. ORNL Patent Section
41. Nuclear Safety Information Center
42. Central Research Library
43. ORNL–Y-12 Technical Library Document Reference Section

EXTERNAL DISTRIBUTION

44. D. E. Bailey, Director, Division of Fuels and Reprocessing, Office of Facilities, Fuel Cycle, and Test Programs, U.S. Department of Energy, Washington, DC 20545
45. F. P. Baranowski, 1110 Dapple Grey Court, Great Falls, VA 22066
46. S. J. Beard, Vice President, Marketing and Uranium Operations, Exxon Nuclear Company, Inc., 600 108th Avenue, N.E., C-00777, Bellevue, WA 98009
47. M. J. Ohanian, Associate Dean for Research, College of Engineering, 300 Weil Hall, University of Florida, Gainesville, FL 32611
48. J. F. Proctor, Senior Technical Specialist, E. I. du Pont de Nemours and Company, Savannah River Laboratory, Aiken, SC 29801
49. Office of Assistant Manager for Energy Research and Development, DOE-ORO, Oak Ridge, TN 37831

50–156. Given distribution as shown in TIC-4500 under UC-86, Consolidated Fuel Reprocessing Category